International Journal of Pharmaceutics 541 (2018) 1–10

Contents lists available at ScienceDirect

International Journal of Pharmaceutics

journal homepage: www.elsevier.com/locate/ijpharm

Preparation of a solid self-microemulsifying drug delivery system by hot-melt extrusion

Luis Antonio D. Silva[a], Susana L. Almeida[a], Ellen C.P. Alonso[a], Priscila B.R. Rocha[a], Felipe T. Martins[b], Luís A.P. Freitas[c], Stephania F. Taveira[a], Marcilio S.S. Cunha-Filho[d], Ricardo N. Marreto[a,*]

[a] Laboratory of Nanosystems and Drug Delivery Devices (NanoSYS), School of Pharmacy, Federal University of Goiás, Goiânia, GO, Brazil
[b] Chemical Institute, Federal University of Goiás, Goiânia, GO, Brazil
[c] School of Pharmaceutical Sciences of Ribeirão Preto, University of São Paulo, Ribeirão Preto, SP, Brazil
[d] Laboratory of Food, Drug and Cosmetics (LTMAC), School of Health Sciences, University of Brasília, Brasília, DF, Brazil

ARTICLE INFO

Keywords:
Carvedilol
Solid SMEDDS
Hot-melt extrusion
Enteric release

ABSTRACT

Hot-melt extrusion (HME) has gained increasing attention in the pharmaceutical industry; however, its potential in the preparation of solid self-emulsifying drug delivery systems (S-SMEDDS) is still unexplored. This study sought to prepare enteric S-SMEDDS by HME and evaluate the effects of the process and formulation variables on S-SMEDDS properties via Box-Behnken design. Liquid SMEDDS were developed, and carvedilol was used as a class II model drug. Mean size, polydispersity index (PdI) and zeta potential of the resulting microemulsions were determined. The extrudates were then obtained by blending the lipid mixture and HPMCAS using a twin-screw hot-melt extruder. SEM, optical microscopy and PXRD were used to characterize the extrudates. *In vitro* microemulsion reconstitution and drug release were also studied. L-SMEDDS gave rise to microemulsions with low mean size, PdI and zeta potential (140.04 ± 7.22 nm, 0.219 ± 0.011 and −9.77 ± 0.86 mV). S-SMEDDS were successfully prepared by HME, and an HMPCAS matrix was able to avoid microemulsion reconstitution and retain drug release in pH 1.2 (12.97%–25.54%). Conversely, microemulsion reconstitution and drug release were gradual in pH 6.8 and complete for some formulations. Extrudates prepared at the lowest drug concentration and highest temperature and recirculation time promoted a complete and rapid drug release in pH 6.8 giving rise to small and uniform microemulsion droplets.

1. Introduction

Lipid-based formulations encompass a wide range of drug delivery systems that present several advantages for oral administration, such as increase drug apparent solubility, enhanced permeability, and reduced pre-systemic metabolism (Feeney et al., 2016; Garg et al., 2016). Cumulatively, this enhances oral bioavailability of poorly water-soluble drugs. In particular, self-microemulsifying drug delivery systems (SMEDDS), which are lipid-based formulations composed of an isotropic mixture of oils, surfactants, and co-surfactants, can produce submicron size o/w emulsions by mild stirring. Furthermore, SMEDDS have displayed clear therapeutic benefits (Pouton and Porter, 2008).

The liquid form of SMEDDS, however, demands the use of soft gelatin capsules (Tang et al., 2008; Singh et al., 2014), which are expensive. The oily material can also leach out of the capsules (Singh et al., 2014). In addition, liquid SMEDDS (L-SMEDDS) may show chemical instability and cause drug precipitation (Singh et al., 2009). In this sense, the use of solid SMEDDS (S-SMEDDS) has been proposed as a more suitable approach (Tan et al., 2013; Tang et al., 2008), reducing production costs and providing stability improvements, better patient compliance, and improvements in dosing accuracy (Singh et al., 2014). Safety can also be improved because solid systems are less irritating to the gastrointestinal mucosa (Tang et al., 2008; Singh et al., 2014).

S-SMEDDS have been prepared by incorporating liquid SMEDDS (L-SMEDDS) into powders using different techniques, such as adsorption on solid carriers (Krupa et al., 2014), wet granulation by high-shear mixer (Franceschinis et al., 2005), spray drying (Yi et al., 2008), extrusion/spheronization (Iosio et al., 2011; Wang et al., 2010), and conventional wet (Deshmukh and Kulkarni, 2014) and melt granulation (Kishore et al., 2015).

Hot-melt extrusion (HME) is an emerging process in the pharmaceutical industry, which has been successfully applied to enhance the

* Corresponding author at: Faculdade de Farmácia UFG, Rua 240, esquina com 5° Avenida, s/n, Setor Leste Universitário, 74 605-170 Goiânia, GO, Brazil.
E-mail address: ricardomarreto@ufg.br (R.N. Marreto).

https://doi.org/10.1016/j.ijpharm.2018.02.020
Received 1 September 2017; Received in revised form 16 January 2018; Accepted 15 February 2018
Available online 16 February 2018
0378-5173/

solubility of poorly water-soluble drugs, allowing high drug loading and content uniformity (Crowley et al., 2007, Thiry et al., 2015). This modern technique shows numerous advantages compared with the processing methods used to produce S-SMEDDS, such as being easily up-scaled, solvent-free, and less time-consuming (Crowley et al., 2007). Until now, there have been no research articles examining the use of hot-melt extrusion for the preparation of S-SMEDDS. Therefore, the feasibility of this method for the production of S-SMEDDS was investigated for the first time. Carvedilol (CARV), a nonselective β-blocker extensively used in clinical practice, was selected as a model drug.

CARV is a pH-dependent poorly water-soluble drug. It has a solubility in phosphate buffer (pH 6.8) that is approximately 10-fold lower than in HCl solution (pH 1.45, 545 μg/mL) (Hamed et al., 2016). This drug undergoes extensive first-pass metabolism in the liver (Giessmann et al., 2004). It is also a substrate for P-glycoprotein (P-gp) in the intestine (Wessler et al., 2013), which reduces its oral bioavailability (~20%) (Benet, 2013). Although a wide range of technologies have been used to improve its biopharmaceutical properties (Planinšek et al., 2011; Shamma and Basha, 2013; Alonso et al., 2016), lipid systems are the most promising alternatives to this drug because they improve both CARV solubility and dissolution, while also promoting drug transport through the lymphatic system and a decrease in P-gp efflux (Mahmoud et al., 2009; Mahmoud et al., 2010; Shah et al., 2014; Singh et al., 2013; Singh et al., 2014, Wei et al., 2005; Venishetty et al., 2012). Thus, a lipid system is the ideal candidate for the proposed study.

This study sought to obtain S-SMEDDS using HME for the first time. Furthermore, the effect of the process and formulation variables on system performance were determined using a Box-Behnken design (BBD).

2. Materials and methods

2.1. Materials

Carvedilol was obtained from Chengtai Shenyang Fine Chemicals Factory (China, > 99%). Capric/caprylic triglycerides (Velsan® CCT, CCT) were obtained from Clariant Chemicals Ltd. (India). Plurol Isostearique® (polyglyceryl-6-isostearate, Plurol) and Transcutol HP® (diethylene glycol monoethyl ether, TransHP) were kindly donated by Gattefossé Corp. (France). AquaSolve AS® LG (hydroxypropyl methylcellulose acetate succinate, HPMCAS) and Klucel® ELF (hydroxypropyl cellulose, HPC) were kindly donated by Ashland Inc. (Brazil). Microcrystalline cellulose pH 101 (MCC) was obtained from Mingtai (Taiwan). Aerosil® 200 Pharma (colloidal silicon dioxide, Aerosil) was obtained from Evonik Degussa GmbH (Essen, Germany), and talc (magnesium silicate, Talc) was obtained from a local pharmacy. Other chemicals and reagents were analytical grade.

2.2. Methods

2.2.1. L-SMEDDS development

The qualitative composition of the L-SMEDDS was determined based on CARV compatibility studies with lipid excipients (Silva et al., 2016; Silva et al., 2017). A series of formulations containing oil (CCT), surfactant (Plurol) and co-surfactant (TransHP) in different ratios (Table 1) were prepared, and 200 μg of each sample was diluted with 300 mL of purified water and kept at 37 °C under mild magnetic stirring. The self-emulsifying capacity of the samples was visually observed after 5 min of magnetic stirring. When necessary, samples were submitted to an additional mixing step in the vortex for 60 s. Next, the mean size and polydispersity index (PdI) of the microemulsions were determined using a Nano S dynamic light scattering (DLS) (Nano S®, Malvern Instruments Ltd., UK). All measurements were performed in triplicate. The appropriate oil/surfactant/cosurfactant ratio was then selected for the preparation of L-SMEDDS containing CARV, which also had its mean size and PdI determined using DLS. Zeta potential was evaluated using a NanoBrook ZetaPlus (Brookhaven, USA) after a 1: 10 dilution in purified water.

Drug solubility in the lipid adjuvants is an important parameter in the L-SMEDDS development, so CARV solubility in pure transcutol and in a 3:1 (m/m) plurol: transcutol mixture was assessed using the flask method (Silva et al., 2017) followed by HPLC analysis (see Section 2.2.3.3). On the other hand, CARV solubility in plurol (a semi-solid adjuvant) was visually assessed using the test tube method (Shete and Patravale, 2013).

2.2.2. Preparation of S-SMEDDS by HME

The constituents of S6 formulation (Table 1) corresponded to 20% (w/w) of the total mass of the solid formulation were accurately weighed and mixed using a mortar and pestle. Then, CARV was added to this mixture (2, 3.5 or 5%, w/w) and homogenized for 2 min. Next, colloidal silicon dioxide (2%, w/w), MCC (30 to 33%, w/w), HPMCAS/HPC (41%, 8: 1 ratio, w/w) and talc (2%) were sequentially added to the mixture, under additional mixing steps of 2 min each.

The resulting mixture (7.5 g) was then fed into a lab-scale vertical twin screw hot-melt extruder (EHM 5, Labmaq do Brasil Ltd., Brazil) using a manual feed hopper. A 16-mm twin screw extruder (L/D = 16) with a helix angle of 1.97° and 24 mm channel width was used. The extruder barrel was equipped with a backflow channel, making recirculation of the molten material possible. The extruded material was collected, cooled to room temperature, and manually cut into small pieces. Extrudates that were 1000–2000 μm in size were used in subsequent studies.

Preliminary tests were performed without recirculation using different screw speeds (50–175 rpm). In addition, different levels of recirculation time were evaluated. Based on the results of preliminary experiments, the independent factors and their levels were selected for a three-factor, three-level, Box-Behnken Design (BBD). This factorial design allows to rationalize the experimental work and it required fewer runs than other factorial designs, such as a central composite design or full designs. The treatment combinations were placed at the midpoints of the edges and at the center of the process space (Abdelbary and AbouGhaly, 2015).

Recirculation time of the molten material (2, 3.5 and 5 min, X_1), temperature gradient applied to the 3 heating zones (100/110/120 °C, 110/120/130 °C or 120/130/140 °C, X_2) and CARV concentration (2, 3.5 and 5%, X_3) were selected as independent variables. Screw speed was fixed at 150 rpm. The dependent variables selected were the % cumulative CARV released in 0.1 M HCl (Y_1) and 0.4 M phosphate buffer (PPB) (Y_2), as well as the reconstitution efficiency (Y_3) and the particle size of the reconstituted droplets (Y_4). The results obtained for each response were fitted to a quadratic polynomial model containing only significant terms. Statistical analysis (ANOVA) and three-dimensional response surface graphs were generated for individual dependent variables. The effects of the independent variables were considered significant when p-values were lower than 0.05. The software Statistica® version 7 was used.

2.2.3. S-SMEDDS characterization

2.2.3.1. Morphological analysis. The morphological characteristics of S-SMEDDS were analysed using a Leica MZ 6 stereomicroscope equipped with a Leica EC 3 camera (0.63x magnification) (Leica Systems, Germany). In addition, the obtained extrudates were submitted to scanning electron microscopy (SEM) analysis, using a JEOL JSM 6610 microscope equipped with EDS model NSS spectral imaging (Thermo Scientific, USA). The materials were coated with gold using a sputter coater Desk V (Denton Vacuum, USA) followed by examination under different magnifications.

2.2.3.2. Powder X-ray diffraction (PXRD). The powdered extrudates and physical mixtures, prepared with or without the oily components were

Table 1
Composition of liquid self-microemulsifying drug delivery systems (L-SMEDDS) and evaluated parameters.

	L-SMEDDS														
	S1	S2	S3	S4	S5	S6	S7	S8	S9	S10	S11	S12	S13	S14	S15
S/CS	1:1	1:1	1:1	1:1	1:1	3:1	3:1	3:1	3:1	3:1	5:1	5:1	5:1	5:1	5:1
O/S_{mix}	1:1	1:2	1:3	1:4	1:5	1:1	1:2	1:3	1:4	1:5	1:1	1:2	1:3	1:4	1:5
O (%, w/w)	50	33.3	25	20	16.6	50	33.3	25	20	16.6	50	33.3	25	20	16.6
S (%, w/w)	25	33.3	37.5	40	41.7	37.5	50	56.3	60	62.6	41.7	55.6	62.5	66.6	69.5
CS (%, w/w)	25	33.3	37.5	40	41.7	12.5	16.7	18.7	20	20.8	8.3	11.1	12.5	13.3	13.9
Emulsification under mild agitation	No	No	No	No	No	Yes	No	No	No	No	Yes	No	No	No	No

O- oil; S- surfactant; CS- cosurfactant; S_{mix}: mixture of surfactant and co-surfactant.

distributed on a sample holder (grooved glass slide) and mounted on the goniometer of a Shimadzu XRD-6000 diffractometer. A graphite monochromatized X-ray beam from a copper anode (CuKα radiation, λ = 0.15418 nm) was produced into a sealed tube at a generator setting of 40 kV and 30 mA. All PXRD profiles were measured at room temperature under a continuous scan mode (θ–2θ scan axis) with a scan speed of 1.000°/min. The intensity data were recorded at each 0.020° in a 2θ range between 5° and 40°. Divergence and scattering slits were used at 1.000°, and a receiving slit (0.300 mm) and counter monochromator were used during data acquisition. The experimental setup and the following data measurements were conducted using the Search Match program (version 4.1) from Shimadzu XRD-6000. The X-ray patterns were dealt as acquired, except for raw data treatment for normalization of all intensities against the most intense one of each diffraction pattern. For each sample, a file containing the normalized intensity data as a function of raw 2θ positions stepped by 0.020° was generated.

2.2.3.3. CARV content. All S-SMEDDS and their physical mixtures were spectrophotometrically assayed for CARV content. To do this, 175 mg of each sample was placed in a 50 mL volumetric flask, and CARV was extracted with methanol in an ultrasonic cleaning bath USC-2899A (Unique, Brazil) for 30 min. Next, the suspension was kept at room temperature for an additional 30 min. Then, the samples were filtered through a 0.45 μm PVDF membrane filter (Milex®, Millipore Corporation Germany), and an aliquot was appropriately diluted with methanol and quantified using a Cary 50 UV–Vis spectrophotometer (Varian, USA) at 241 nm. The experiments were conducted in triplicate. The extraction procedure was previously validated, and CARV recovery was 101.09% ± 1.30. Extrudates containing no CARV (blank) were submitted to the same extraction protocol and the resulting solutions were used as a blank in the UV–VIS analysis.

Since CARV degradants can influence the results of a UV–VIS analysis, the CARV content of extrudates obtained in the condition with the highest temperature and longest recirculation time (F4, Table 3) was assessed using a validated stability-indicating HPLC method. The HPLC system (Agilent 1260 Infinity II) consisted of a quaternary pump (G7111B), autosampler (G7129A), and UV detector (G7114A), all of which were obtained from Agilent Technologies (USA). Separation was achieved using an Agilent ZORBAX Eclipse XDB-C18 (150 × 3.0 mm, 5 μm) with a short guard column (12.5 × 4.6 mm, 5 μm; Agilent) maintained at 30 °C. The mobile phase consisted of a 50-mM phosphate buffer: methanol mixture (40: 60, v/v, pH 4) with a flow rate of 1.0 mL min^{-1} and injection volume of 20 μL. Detection was carried out at 241 nm. The analytical curve was linear ($r^2 = 1$) in the concentration range of 50–1600 ng mL^{-1}. The method was found to be accurate (96.9–101.5%) and precise (CV 3.84%) with a quantification limit of 50 ng mL^{-1}. Selectivity was investigated (formulation components), and no interference was observed in drug retention time. Furthermore, the peak area did not change in the presence of these products.

Table 2
Unloaded and drug loaded liquid self-microemulsifying drug delivery systems (L-SMEDDS) S6.

Parameters	Unloaded-L-SMEDDS	CARV-L-SMEDDS
Particle size (nm)	140.04 ± 7.22	139.06 ± 7.28
PdI	0.219 ± 0.011	0.221 ± 0.015
Zeta Potential (mV)	−9.77 ± 0.86	−4.99 ± 0.45*
Transmittance (%) at 850 nm	35.83 ± 2.84	37.15 ± 2.13

* Significant difference ($p < 0.05$) between zeta potential values of unloaded and loaded L-SMEDDS.

2.2.3.4. In vitro drug release. *In vitro* drug release experiments were performed, as described by Zecevic et al. (2014), with some modifications. Briefly, 175 mg of the S-SMEDDS formulations which are equivalent to 3.5, 6.125 or 8.75 mg of CARV (2%, 3.5% or 5% of the drug, respectively), were placed in glass cubes of a VK 7000 dissolution system (VARIAN, USA). Physical mixtures and the pure drug were also assessed. The tests were undertaken with a USP apparatus II at 37 °C. At the first 2 h of the experiment, the dissolution medium was 375 mL of 0.1 M HCl solution (pH 1.2). Next, the pH of the medium was adjusted to 6.8 with a proper amount of 0.2 M potassium hydroxide solution and 0.4 M potassium phosphate buffer (PPB). The total medium volume was 900 mL, and the experiment was carried out for an additional 3 h. The samples were withdrawn at predetermined time intervals, filtered through a 0.45 μm PVDF membrane and analysed using a Cary 50 UV–VIS spectrophotometer (Varian, USA) at 241 nm. The analytical curves were prepared with CARV solutions in 0.1 M HCl and 0.4 M PPB. The experiments were performed under sink conditions (n = 3). Statistical analysis was performed considering the % drug dissolved at 120 min (acidic condition), and at 300 min (pH 6.8) using GraphPad Prism 5 Software (La Jolla, USA). ANOVA, followed by Tukey's multiple comparison tests, was used.

2.2.3.5. Reconstitution efficiency. The emulsification behaviour of the S-SMEDDS was investigated by adding 1 g of the extrudates (corresponding to 0.2 g of L-SMEDDS) in a glass beaker containing 300 mL of 0.4 M PPB, pH 6.8. The medium was kept under magnetic stirring (100 rpm) at 37 °C for 3 h. Five-millilitre samples were withdrawn at predetermined time intervals, centrifuged for 5 min at 3000*g* in a Sigma 3–18 k centrifuge (SciQuip, UK), and filtered through a 0.45 μm PVDF membrane. The filtrate was then analysed for transmittance (T%) at 850 nm, using a Cary 50 UV–vis spectrophotometer (Varian, USA) (Nikolakakis and Malamataris, 2014). Once analysed, the samples were returned to the reconstitution medium. An extrudate prepared without adding oil and surfactants was also evaluated and the T% value measured was deducted from S-SMEDDS analysis to exclude any interference caused by the medium and other constituents of the formulation (Matsaridou et al., 2012). The same protocol was used to determine the reconstitution in 0.1 M HCl after 2 h as well as the transmittance of the L-SMEDDS. The reconstitution efficiency (RE%) was calculated according to Eq. (1):

Table 3
Box-Behnken experimental matrix and observed responses.

Runs	X_1	X_2	X_3	Y_1	Y_2	Y_3	Y_4
F1	5	110	2	18.53 ± 1.72	81.68 ± 3.10	100.32 ± 0.68	155.03 ± 2.43
F2	3.5	110	3.5	19.00 ± 2.09	57.08 ± 1.30	90.55 ± 1.48	154.46 ± 4.44
F3	3.5	120	2	14.36 ± 1.53	85.54 ± 1.79	89.18 ± 2.09	161.93 ± 3.95
F4	5	120	3.5	12.97 ± 0.52	72.04 ± 1.71	90.11 ± 0.91	154.23 ± 1.25
F5	3.5	120	5	17.65 ± 0.14	50.20 ± 2.38	70.99 ± 1.34	164.72 ± 2.29
F6	2	100	3.5	23.55 ± 1.44	52.22 ± 1.96	69.16 ± 1.15	153.73 ± 2.47
F7	5	110	5	17.44 ± 0.51	60.32 ± 0.50	75.03 ± 0.41	150.10 ± 6.20
F8	3.5	100	5	24.27 ± 0.40	43.62 ± 1.31	55.66 ± 1.34	156.86 ± 3.91
F9	2	110	2	18.40 ± 1.88	83.31 ± 6.88	88.56 ± 0.22	163.30 ± 2.76
F10	2	120	3.5	17.44 ± 0.56	73.86 ± 0.52	88.45 ± 1.16	156.46 ± 0.63
F11	5	100	3.5	25.54 ± 0.77	57.66 ± 0.33	81.15 ± 1.37	148.96 ± 7.82
F12	2	110	5	19.43 ± 0.72	45.75 ± 0.44	66.35 ± 2.40	145.63 ± 2.00
F13	3.5	110	3.5	19.66 ± 2.10	57.14 ± 2.11	91.10 ± 1.67	152.80 ± 2.08
F14	3.5	100	2	25.18 ± 0.95	74.18 ± 3.74	91.75 ± 1.02	157.36 ± 2.27
F15	3.5	110	3.5	18.60 ± 0.76	54.57 ± 1.14	91.99 ± 1.33	152.10 ± 3.99

Independent variables: Recirculation time (X1), temperature at the first heating zone (X2) and CARV concentration (X3). Dependent variables: cumulative % CARV released in HCl medium (Y_1), cumulative % CARV released in PPB medium (Y_2), reconstitution efficiency in PPB (Y_3), mean size of the reconstituted droplets (Y_4). Data are presented as the mean ± SD (n = 3).

$$RE\% = \frac{(\%T_{SS} - \%T_B) \times 100}{TSL - \%T_B} \quad (1)$$

where T_{ss} is the % transmittance of the reconstituted S-SMEDDS, T_B is the % transmittance of the blank, and T_{SL} is the % transmittance of L-SMEDDS. Statistical analysis was performed considering the RE% values of the samples withdrawn at 180 min of the experiment (pH 6.8) using GraphPad Prism 5 Software (La Jolla, USA). ANOVA, followed by Tukey's multiple comparison tests, was used. The mean diameter and PdI of the reconstituted droplets were evaluated, as described in section 2.2.1. The experiments were performed in triplicate with the results expressed as the mean ± SD.

3. Results and discussion

3.1. L-SMEDDS characterization

The different combinations of CCT (oil), Plurol (surfactant) and TransHP (co-surfactant) led to the formation of translucent microemulsions with mean size values ranging from 116.2 ± 12.1 nm to 149.2 ± 30.2 nm, without any significant differences between them ($p > 0.05$). PdI values ranged from 0.29 ± 0.03 to 0.38 ± 0.06 ($p > 0.05$), denoting the occurrence of a uniform size distribution in the samples. Formulations S6 and S11 (Table 1) resulted in microemulsions in less than 60 s upon mild stirring, whereas the other formulations resulted in microemulsions only after an additional mixture step involving the use of a vortex stirrer.

Formulation S6 was then selected for further studies since it has a greater amount of hydrophilic surfactant compared to S11, which could be interesting for producing more stable o/a microemulsions.

CARV solubility in CCT was 3.93 mg mL^{-1} (Silva et al., 2017). On the other hand, CARV solubility in transcutol and plurol was 120.22 mg mL^{-1} and 6 mg mL^{-1}, respectively. A mixture of plurol: transcutol prepared at a 3:1 ratio (as seen in S6) solubilized 38.22 mg mL^{-1} of CARV. Regardless, monophasic systems were only observed when CARV was added at 20 mg mL^{-1} to S6, which again resulted in rapid microemulsion formation with no drug precipitation after dilution in aqueous media (pH 6.8).

The microemulsion droplets of the CARV-loaded S6 formulation displayed similar mean sizes and PdI values compared to the unloaded L-SMEDDS samples ($p > 0.05$) (Table 2). Conversely, the surface charge of the droplets showed a significant decrease ($p < 0.05$) due to CARV incorporation. This can be attributed to the positive residual charge of the CARV amine group at pH 6.8. The %T value of unloaded and drug loaded microemulsions were similar ($p > 0.05$) (Table 2). Altogether, these results indicated that drug incorporation in the selected L-SMEDDS did not negatively impact its self-emulsifying properties.

3.2. S-SMEDDS production by hot-melt extrusion

Preliminary tests were performed to determine the ranges of extruder operating conditions and the basic composition of the formulation in order to guarantee an adequate extrusion process as well as the ability of the extrudates to reduce drug release in an acidic medium. First, unsuccessful attempts using mixtures of CARV, HPMCAS, MCC, talc, and colloidal silicon dioxide were performed in the range of 100–140 °C and under different processing conditions. The addition of the solid plasticizer HPC (Zecevic et al., 2014), which was adjusted to a mass ratio of 8:1 HPMCAS: HPC, made possible the extrusion of the formulation using up to 20% (w/w) of an oil/surfactant mixture.

Based on these preliminary findings, the formulations were processed without molten recirculation and using different screw speeds (50–175 rpm). The extrudates obtained showed fast disintegration in HCl 0.1 N (data not shown), suggesting the poor mixing of the HPMCAS in the matrix regardless of the screw speed used. In an attempt to promote better polymer distribution in the matrix, extrudates were then prepared using different recirculation times at a screw speed of 150 rpm. Only extrudates obtained with more than 2 min of recirculation retained structural integrity in the HCl medium, which demonstrated the need for a sufficient recirculation time in order to guarantee proper distributive mixing in this process. Similarly, Renterghem et al. (2017) found that the recirculation of molten material was a key factor for achieving proper distributive mixing in mini extruders. Therefore, recirculation time, temperature, and CARV concentration were selected for the Box-Behnken design as independent factors.

All tested conditions in the Box-Behnken design (Table 3) led to the formation of extrudates with a smooth surface and a homogeneous and dense structure (Fig. 1). No oil separation was seen during the hot-melt extrusion. A close view of the cut extrudates (Fig. 1j, 1 k and 1 L) shows some dark spots on their surface, which can be attributed to the presence of oily constituents.

The CARV physical state in the extrudates and physical mixtures were investigated using PXRD. The standard diffractogram of pure CARV and its physical mixtures prepared at different CARV concentrations and without oil addition are shown in Fig. 2. Neat crystalline CARV presented the characteristic PXRD patterns (Planinšek et al., 2011). CARV diffraction peaks could only be detected in the physical mixtures containing 5% and 10% (w/w) CARV since no CARV peak with an intensity higher than average intensity of the corresponding

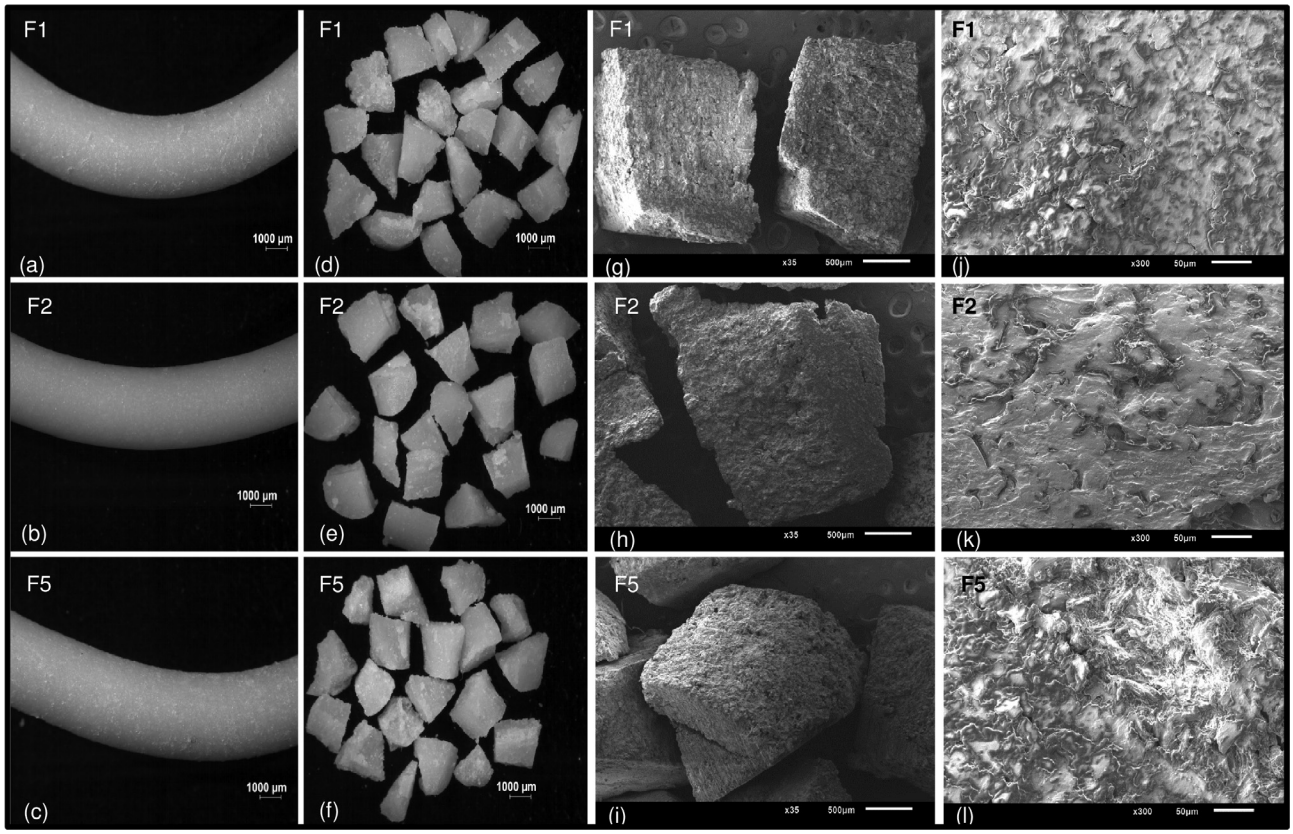

Fig. 1. Optical and electron micrographs of the F1 (CARV 2%), F2 (CARV 3.5%) and F5 (CARV 5%) extrudates from Table 3. Optical micrographs of the whole (a, b and c) and cut extrudates (d, e and f) (×0.63 magnification) and scanning electron micrographs of the cross-section of the cut extrudates at ×35 (g, h and i) and ×300 (j, k and l) magnification.

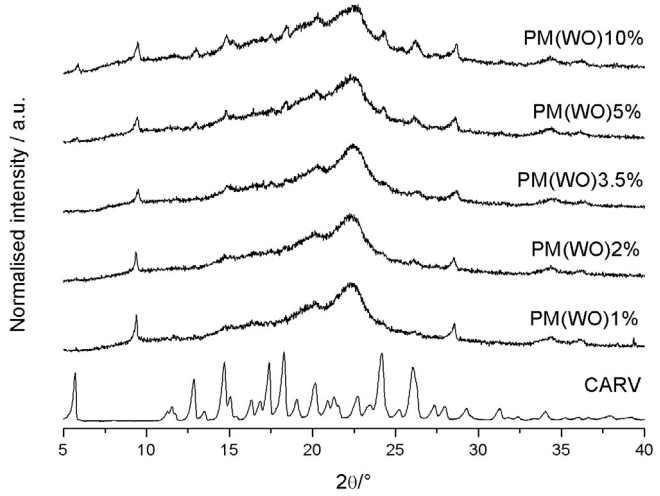

Fig. 2. Powder X-ray diffractograms of pure CARV and its physical mixtures (PM 1%, 2%, 3.5%, 5% and 10% of CARV) prepared without oil (WO) addition.

diffractogram baseline, plus three times its standard uncertainty, were found in the PXRD profiles of the physical mixtures containing 1%, 2% and 3.5% of CARV (Fig. 2). These findings suggested that CARV peaks could not be detected by PXRD when the drug concentration was lower than 5%.

Fig. 3 (a, b, and c) shows the standard diffractograms of pure CARV, physical mixtures prepared with oil and powdered S-SMEDDS formulations obtained in the BBD (Table 3). Only two diffraction peaks at 9.5° and 28.5° (in 2θ) could be seen in the PXRD patterns, which can be attributed to the presence of colloidal silicon dioxide in the samples. The absence of the characteristic CARV peaks in the physical mixture containing oil and 5% CARV suggested that a certain drug amount was dissolved in this material. S-SMEDDS diffractograms showed no peaks related to crystalline CARV, which could be a result of the formation of amorphous CARV together with its solubilization by the oily constituents.

3.3. Effect of formulation and process factors on performance of the S-SMEDDS

Fifteen extrudates were obtained according to the Box-Behnken design (Table 3). CARV content in all extrudates ranged from 92.24 to 102.57%, which was determined by UV–VIS spectrometry. The coefficients of variation were less than 2%, indicating good content uniformity in the samples. CARV content was also assessed using a validated HPLC method in order to exclude the possible interference of CARV degradation products in the UV–VIS analyses. The chromatographic analysis performed with the extrudate obtained under the highest temperature and longest recirculation time in the Box-Behnken design (F4, Table 3) showed a CARV content of 94.71% ± 5.17%, proving that the drug remained stable after the HME process. A typical chromatogram obtained from the analysis of the blank and the drug-loaded extrudate is shown in Fig. 4.

% CARV released in the HCl medium (120 min) was in the range from 12.97 ± 0.52% to 25.54 ± 0.77% (Table 3), and all the S-SMEDDS structures remained intact after the dissolution period in an acid medium (120 min). This result proved the effect of the enteric polymer in retarding the drug release. HPMCAS is a cellulose derivative with pH-dependent solubility, and its presence in the extrudates may avoid the premature CARV release in the stomach, which could potentiate drug absorption by the lymphatic route in the intestine. HME give rise to low-porosity materials (Stanković et al., 2015), which is a key factor in reaching a strict control of drug release from a matrix

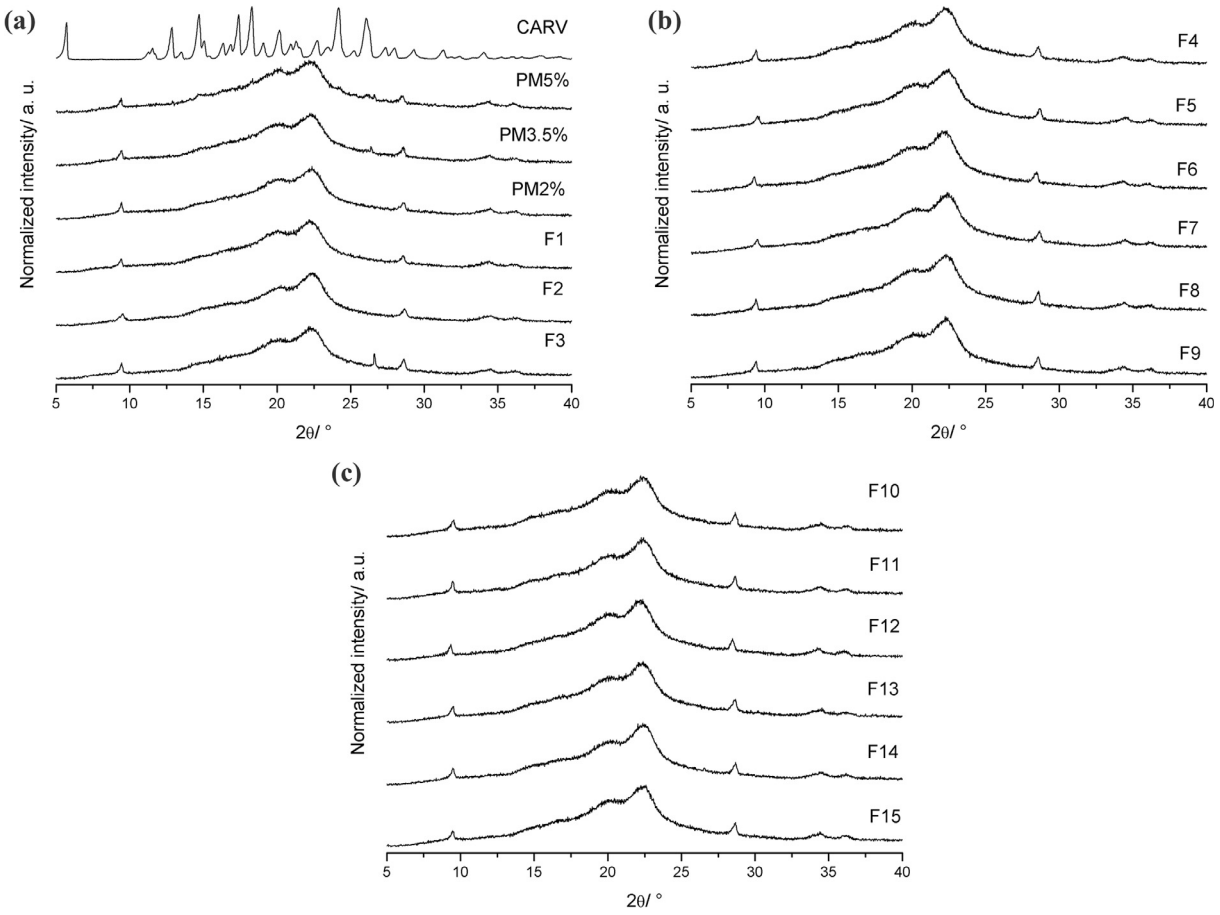

Fig. 3. Diffractograms of pure CARV, physical mixtures (PM 2%, 3.5% and 5% of CARV) and S-SMEDDS (formulations F1 to F15, Table 3). (a) PM and F1 to F3; (b) F4 to F9; (c) F10 to F15.

system. Fig. 5 shows the drug release profile of all S-SMEDDS formulations. On the other hand, the percentage of CARV released from the physical mixtures was approximately 60% in 30 min (HCl, pH 1.2), whereas pure CARV dissolved by only 20% over the same time period. These data suggest that the microemulsion formation affects the amount of CARV released from the physical mixtures. Additionally, the comparison between CARV released from the physical mixtures and extrudates clearly demonstrates a role for HME processing in reducing drug release in an HCl medium.

Statistical analysis showed that the drug released in HCl pH 1.2 was

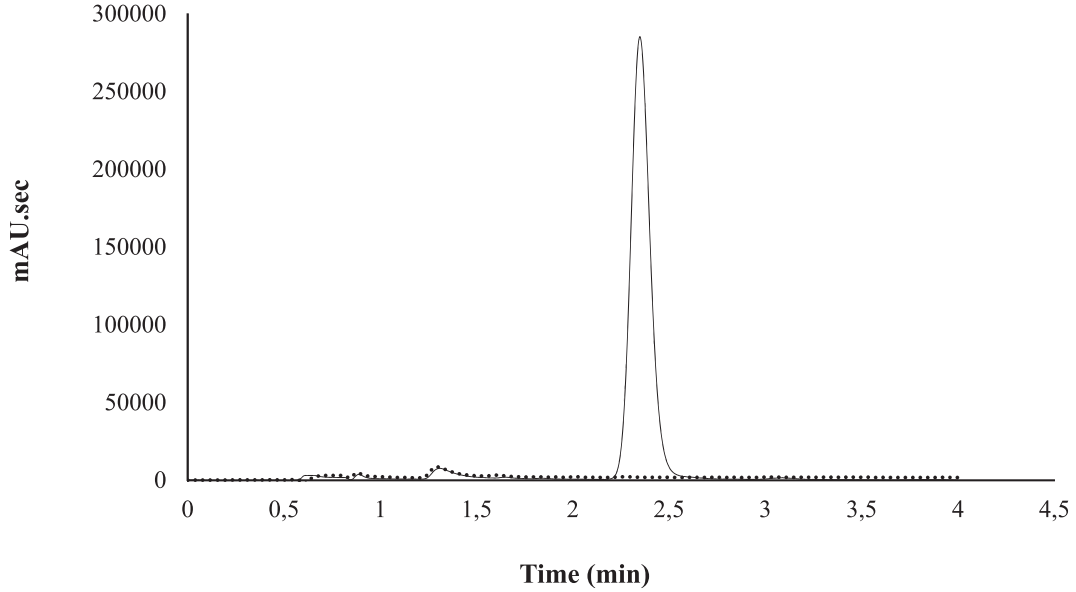

Fig. 4. Overlaid HPLC chromatograms of blank and CARV-loaded extrudate (F4, Table 3). C18 column (150 × 3.0 mm, 5 µm), mobile phase consisted of a 50-mM phosphate buffer: methanol mixture (40: 60, v/v, pH 4) with a flow rate of 1.0 mL min^{-1} and injection volume of 20 µL, oven temperature at 30 °C, and detection at 241 nm.

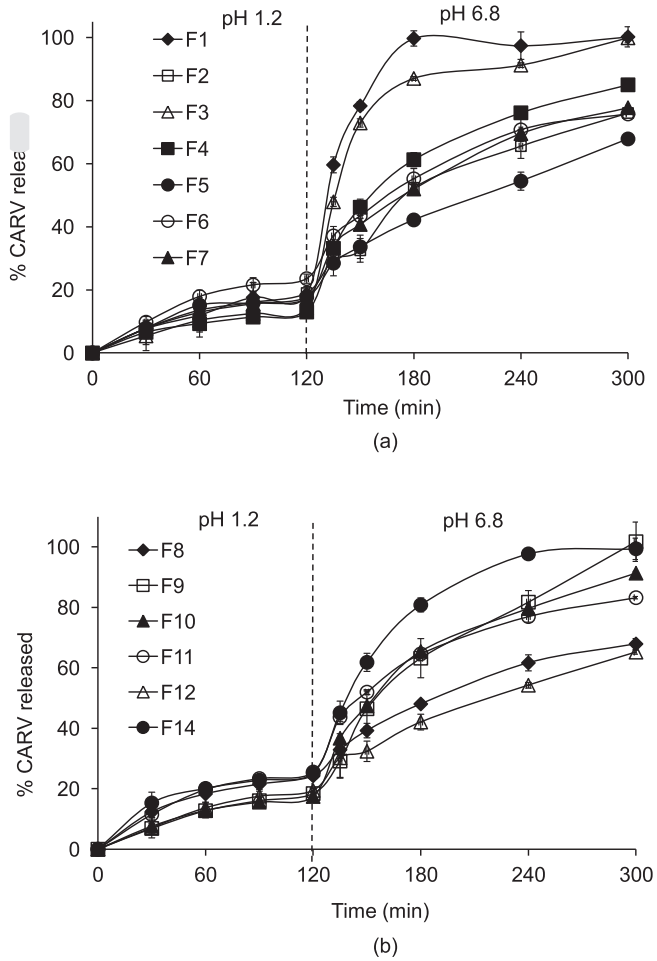

Fig. 5. *In vitro* CARV release profiles from the S-SMEDDS in 0.1 M HCl pH 1.2 (0–120 min) and 0.4 M PPB pH 6.8 (120–300 min). (a) formulations 1 to 7; (b) formulations 8 to 14.

significantly reduced when recirculation time (X_1) and temperature (X_2) were increased (Fig. 6a). The interactions between these two factors (X_1X_2) and the quadratic term of temperature (X_2^2) also significantly affected this response ($p < 0.05$). The effects of the significant variables can be attributed to a better polymer dispersion in the matrix, probably because of a decrease in melt viscosity and superior homogenization. Conversely, CARV concentration did not have a significant effect on a drug released at pH 1.2, but this factor showed a significant interaction with temperature (X_2X_3). At a higher temperature, an increase in the drug concentration resulted in a higher drug release.

CARV released in pH 6.8 (300 min of experiment) ranged from 43.62 ± 1.31% to 85.54 ± 1.79% (Table 3). For some formulations, the drug release reached 100% of the expected theoretical amount, considering the amount of CARV released in HCl and PPB (Fig. 5).

Fig. 6b depicts the surface plot of the % drug released at 300 min as a function of the drug concentration and temperature. Statistical analysis showed that CARV release at pH 6.8 was significantly reduced when its concentration (X_3) was increased, which can be explained by the CARV limited solubility in the self-emulsifying mixture. Therefore, an increase in drug concentration probably led to a higher CARV amount in the polymeric matrix (in the amorphous or crystalline state) than dissolved in the lipid adjuvants. PXRD was used to detect crystalline CARV in the samples (section 3.2); however, the detection limit was found to be 5% (m/m) of CARV; therefore, it was not possible to identify the presence of a CARV crystalline fraction in the samples (extrudates or physical mixtures containing oil). Similarly, Seo et al. (2003) prepared agglomerates containing lactose monohydrate, polyethylene glycol 3000 or Gelucire® 50/13 and diazepam by melt agglomeration in a high shear mixer. These authors showed that the higher dissolution rates were seen at lower drug concentrations, suggesting a higher degree of molecular dispersion in these formulations.

Conversely, an increase in the recirculation time and processing temperature caused an increase in drug release (Fig. 6c), which can be attributed to the improvement of drug solubilization in the oil/surfactant mixture at high levels of these factors, as well as to a higher formation of amorphous CARV in the polymeric matrix. These results are in agreement with those discussed in a previous study (Seo et al., 2003). The interaction between the recirculation time and concentration (X_1X_3) also affected CARV release ($p < 0.05$). In Fig. 6c, recirculation

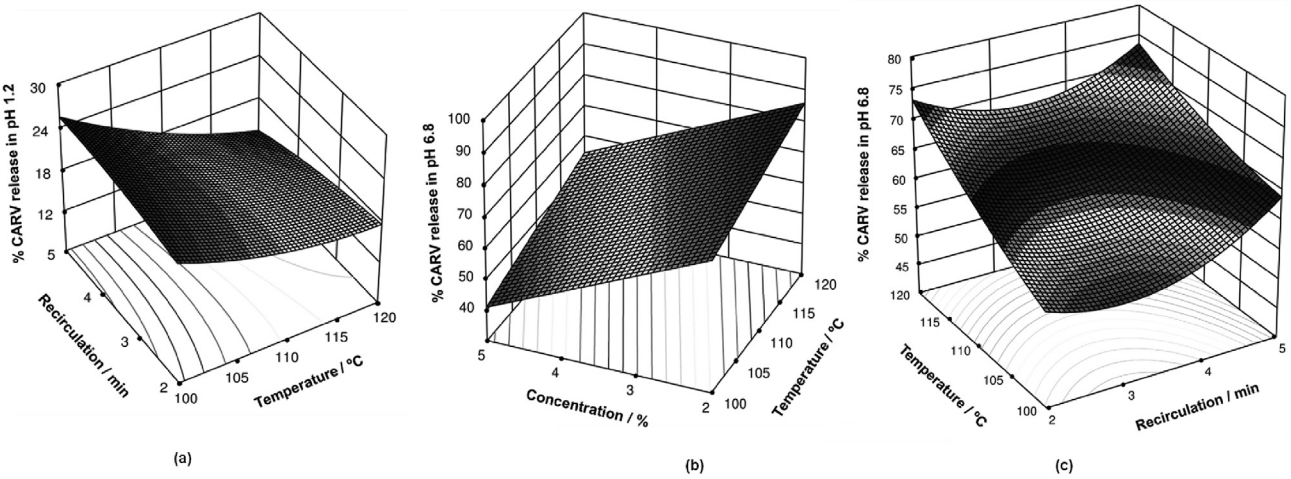

(a) $y = 19.563 - 1.085X_1 - 9.030X_2 - 3.230X_1X_2 + 2.100\ X_2X_3 - 1.351X_2^2$

(b) and (c) $y = 65.031 + 13.490X_2 - 31.205X_3 + 8.100X_1X_3 + 6.030X_1^2 - 5.470X_3^2$

Fig. 6. Response surface plots showing the effects of independent variables on the cumulative % CARV released in HCl pH 1.2 (a), and PPB pH 6.8 (b, c), and its respective adjusted polynomial equations. Recirculation time (X1), temperature at the first heating zone (X2) and CARV concentration (X3).

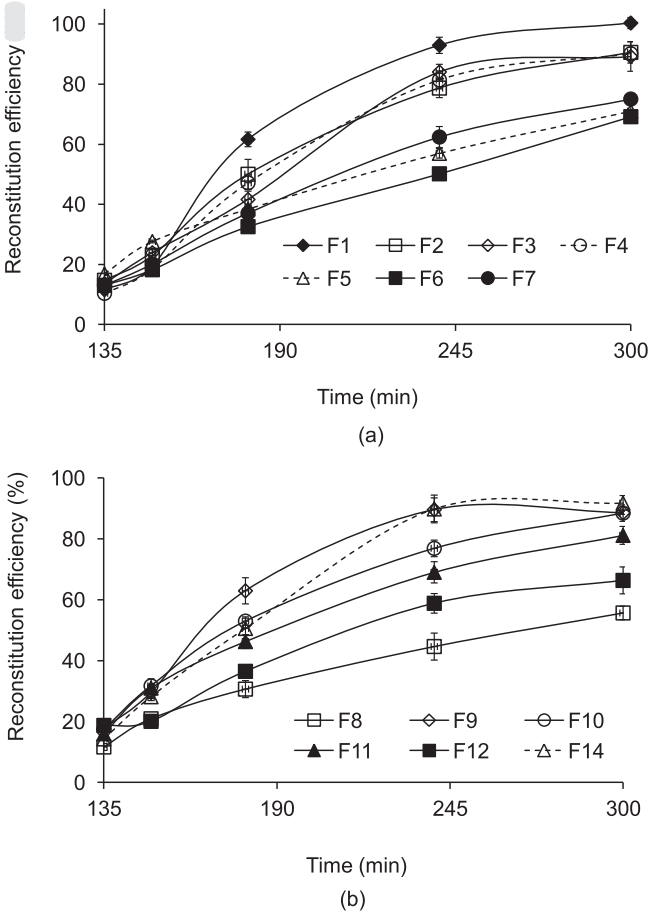

Fig. 7. Reconstitution efficiency (%) from S-SMEDDS in pH 6.8. (a) formulations 1 to 7; (b) formulations 8 to 14.

time was shown to have a significant quadratic effect. Additionally, higher temperatures at high or low recirculation levels potentiate the drug release at pH 6.8.

The reconstitution efficiency (RE%) of S-SMEDDS was evaluated based on the transmittance (%T) of the dispersions prepared by adding the extrudates in phosphate buffer at a pH 6.8 and HCl at a pH 1.2, according to Eq. (1). Droplet size and PdI were also evaluated by DLS. For all extrudates, the %T values in HCl at a pH 1.2 were constant and equal to the %T values of the HCl solution, which means no microemulsion reconstitution occurred due to the effect of the enteric polymer.

In contrast, RE% values in the PPB medium ranged from 55.66% ± 1.34 to 100.32% ± 0.28 (Table 3). Fig. 7 shows a gradual increase in RE% values, suggesting a slow solvent penetration in the extrudates. In addition, intermolecular interactions between the self-emulsifying constituents and solid excipients can significantly affect the reconstitution (Matsaridou et al., 2012; Nikolakakis and Malamataris, 2014).

The reconstitution of the microemulsion plays an important role in the development of S-SMEDDS since it is necessary to ensure the maintenance of the emulsification properties, while the droplet size and PdI values should be similar to those observed for the corresponding liquid systems (Nikolakakis and Malamataris, 2014; Yi et al., 2008).

ANOVA analysis was performed from the reconstitution efficiency (%) at 300 min. An increase in the recirculation time (X_1) and processing temperature (X_2) led to an increase in the RE%, whereas the drug concentration (X_3) showed the opposite effect. These effects can be seen in Fig. 8. The interaction between temperature and drug concentration and the quadratic term of temperature and drug concentration also showed a significant effect ($p < 0.05$) on RE%.

An increase in temperature probably caused a higher distribution of the lipid constituents in the solid matrix due to a decrease in the melt viscosity. Similarly, a better mechanical homogenization under higher recirculation time is suggested to increase the oil distribution in the extrudates. Reconstitution data agree with the drug release data, suggesting that the drug release was mostly related to the self-emulsifying properties of the S-SMEDDS.

It has been reported that the drug type may affect the microemulsion properties and stability (Nikolakakis et al., 2015; Singh et al.,

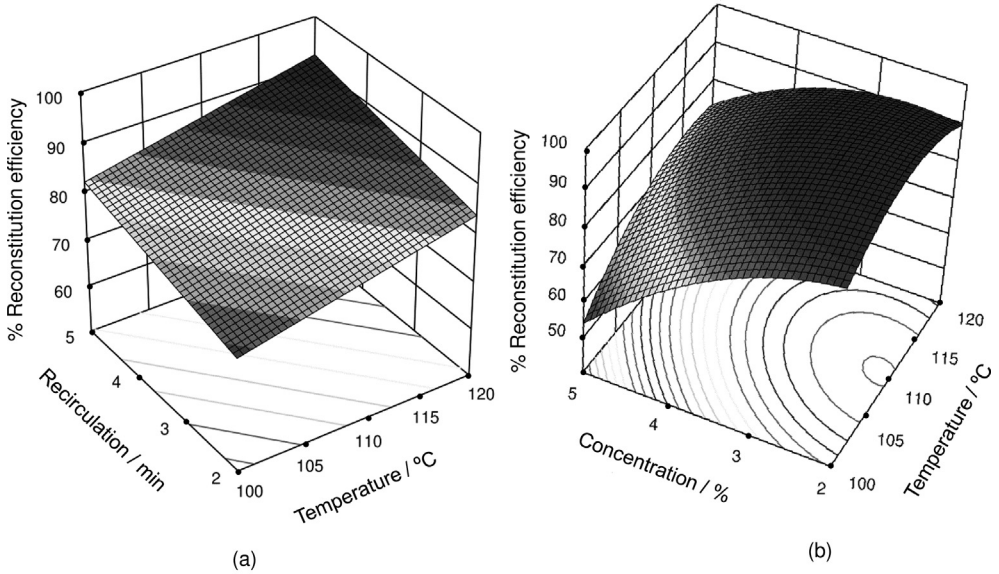

$$y = 80.565 + 8.523X_1 + 10.255X_2 - 25.446X_3 + 8.947X_2X_3 + 7.330X_2^2 + 6.985X_3^2$$

Fig. 8. Response surface plots showing the effects of independent variables on the percentage of reconstitution efficiency at pH 6.8, and the adjusted polynomial equation. (a) effects of recirculation time and temperature; (b) effects of CARV concentration and temperature. Recirculation time (X1), temperature at the first heating zone (X2) and CARV concentration (X3).

2013). In the present study, an increase in drug concentration led to a reduction in RE% values. This can be attributed to an increase in the melt viscosity in the formulations containing a higher drug concentration, which hampers the liquid distribution in the solid matrix. The oily phase migration rate has been reported to significantly decrease due to drug incorporation in a solid matrix containing inert emulsions (Nikolakakis and Malamataris, 2014).

The mean diameter of the reconstituted droplet and the PdI values should also be considered in S-SMEDDS development. Agglomeration or size increase are not expected to occur during reconstitution. The mean size and PdI values of the reconstituted microemulsions at 300 min ranged from 145.63 ± 2.00 nm to 164.72 ± 2.29 nm and from 0.209 ± 0.006 to 0.262 ± 0.004, respectively (Table 3). Droplet mean size was used as a response in the Box-Behnken design, but none of the independent variables studied affected these data significantly. Therefore, size and PdI values remained unchanged in the reconstituted dispersions compared to L-SMEDDS ($p > 0.05$).

4. Conclusion

L-SMEDDS composed of CCT, Plurol and TransHP (50/37.5/12) gave rise to a clear, translucent microemulsion upon gentle stirring with water. This formulation was incorporated in an enteric polymeric matrix based on HPMCAS using HME. Box-Behnken design and ANOVA analysis showed that the lowest CARV concentration and the highest temperature and recirculation time during HME led to a rapid and complete microemulsion reconstitution and drug release in pH 6.8, whereas it reduced drug release and avoided reconstitution in acidic conditions.

This is the first report on the effect of the process and formulation variables upon the quality attributes of S-SMEDDS prepared by HME, which is a versatile, industrially viable and solvent-free process that has attracted increasing attention from the pharmaceutical industry.

Acknowledgements

This research was supported by the Brazilian agencies CNPq and CAPES Additionally, the authors thank Ashland for kindly supplying the polymers used in the study. We also thank the coordinator of the FARMATEC-UFG, Prof. Eliana M. Lima, for the necessary facilities and the LABMIC-UFG for the SEM analysis.

References

Abdelbary, A.A., AbouGhaly, M.H.H., 2015. Design and optimization of topical methotrexate loaded niosomes for enhanced management of psoriasis: application of Box-Behnken design, in-vitro evaluation and in-vivo skin deposition study. Int. J. Pharm. 485, 235–243. http://dx.doi.org/10.1016/j.ijpharm.2015.03.020.

Alonso, E.C.P., Riccomini, K., Silva, L.A.D., Galter, D., Lima, E.M., Durig, T., Taveira, S.F., Martins, F.T., Cunha-Filho, M.S.S., Marreto, R.N., 2016. Development of carvedilol-cyclodextrin inclusion complexes using fluid-bed granulation: a novel solid-state complexation alternative with technological advantages. J. Pharm. Pharmacol. 68, 1299–1309. http://dx.doi.org/10.1111/jphp.12601.

Benet, L.Z., 2013. The role of BCS (Biopharmaceutics classification system) and BDDCS (biopharmaceutics drug disposition classification system) in drug development. J. Pharm. Sci. 102, 34–42. http://dx.doi.org/10.1002/jps.23359.

Crowley, M.M., Zhang, F., Repka, M.A., Thumma, S., Upadhye, S.B., Battu, S.K., McGinity, J.W., Martin, C., 2007. Pharmaceutical applications of hot-melt extrusion: Part I. Drug Dev. Ind. Pharm. 33, 909–926. http://dx.doi.org/10.1080/03639040701498759.

Deshmukh, A., Kulkarni, S., 2014. Solid self-microemulsifying drug delivery system of ritonavir. Drug Dev. Ind. Pharm. 40, 477–487. http://dx.doi.org/10.3109/03639045.2013.768632.

Feeney, O.M., Crum, M.F., McEvoy, C.L., Trevaskis, N.L., Williams, H.D., Pouton, C.W., Charman, W.N., Bergström, C.A.S., Porter, C.J.H., 2016. 50 years of oral lipid-based formulations: provenance, progress and future perspectives. Adv. Drug Deliv. Rev. 101, 167–194. http://dx.doi.org/10.1016/j.addr.2016.04.007.

Franceschinis, E., Voinovich, D., Grassi, M., Perissutti, B., Filipovic-Grcic, J., Martinac, A., Meriani-Merlo, F., 2005. Self-emulsifying pellets prepared by wet granulation in high-shear mixer: influence of formulation variables and preliminary study on the *in vitro* absorption. Int. J. Pharm. 291, 87–97. http://dx.doi.org/10.1016/j.ijpharm.2004.07.046.

Garg, N.K., Tyagi, R.K., Singh, B., Sharma, G., Nirbhavane, P., Kushwah, V., Jain, S., Katare, O.P., 2016. Nanostructured lipid carrier mediates effective delivery of methotrexate to induce apoptosis of rheumatoid arthritis via NF-κB and FOXO1. Int. J. Pharm. 499, 301–320. http://dx.doi.org/10.1016/j.ijpharm.2015.12.061.

Giessmann, T., Modess, C., Hecker, U., Zschiesche, M., Dazert, P., Kunert-Keil, C., Warzok, R., Engel, G., Weitschies, W., Cascorbi, I., Kroemer, H.K., Siegmund, W., 2004. CYP2D6 genotype and induction of intestinal drug transporters by rifampin predict presystemic clearance of carvedilol in healthy subjects. Clin. Pharmacol. Ther. 75, 213–222. http://dx.doi.org/10.1016/j.clpt.2003.10.004.

Hamed, R., Awadallah, A., Sunoqrot, S., Tarawneh, O., Nazzal, S., Al Baraghthi, T., Al Sayyad, J., Abbas, A., 2016. pH-dependent solubility and dissolution behavior of carvedilol—case example of a weakly basic BCS class II drug. AAPS PharmSciTech. 17, 418–426. http://dx.doi.org/10.1208/s12249-015-0365-2.

Iosio, T., Voinovich, D., Perissutti, B., Serdoz, F., Hasa, D., Grabnar, I., Dall' Acqua, S., Zara, G.P., Muntoni, E., Pinto, J.F., 2011. Oral bioavailability of silymarin phytocomplex formulated as self-emulsifying pellets. Phytomedicine 18, 505–512. http://dx.doi.org/10.1016/j.phymed.2010.10.012.

Kishore, R.N., Yalavarthi, P.R., Vadlamudi, H.C., Vandana, K.R., Rasheed, A., Sushma, M., 2015. Solid self microemulsification of atorvastatin using hydrophilic carriers: a design. Drug Dev. Ind. Pharm. 41, 1213–1222. http://dx.doi.org/10.3109/03639045.2014.938655.

Krupa, A., Jachowicz, R., Kurek, M., Figiel, W., Kwiecień, M., 2014. Preparation of solid self-emulsifying drug delivery systems using magnesium aluminometasilicates and fluid-bed coating process. Powder Technol. 266, 329–339. http://dx.doi.org/10.1016/j.powtec.2014.06.043.

Mahmoud, E.A., Bendas, E.R., Mohamed, M.I., 2010. Effect of formulation parameters on the preparation of superporous hydrogel self-nanoemulsifying drug delivery system (SNEDDS) of carvedilol. AAPS PharmSciTech. 11, 221–225. http://dx.doi.org/10.1208/s12249-009-9359-2.

Mahmoud, E.A., Bendas, E.R., Mohamed, M.I., 2009. Preparation and evaluation of self-nanoemulsifying tablets of carvedilol. AAPS PharmSciTech. 10, 183–192. http://dx.doi.org/10.1208/s12249-009-9192-7.

Matsaridou, I., Barmpalexis, P., Salis, A., Nikolakakis, I., 2012. The influence of surfactant HLB and oil/surfactant ratio on the formation and properties of self-emulsifying pellets and microemulsion reconstitution. AAPS PharmSciTech. 13, 1319–1330. http://dx.doi.org/10.1208/s12249-012-9855-7.

Nikolakakis, I., Malamataris, S., 2014. Self-emulsifying pellets: relations between kinetic parameters of drug release and emulsion reconstitution—influence of formulation variables. J. Pharm. Sci. 103, 1453–1465. http://dx.doi.org/10.1002/jps.23919.

Nikolakakis, I., Panagopoulou, A., Salis, A., Malamataris, S., 2015. Relationships between the properties of self-emulsifying pellets and of the emulsions used as massing liquids for their preparation. AAPS PharmSciTech. 16, 129–139. http://dx.doi.org/10.1208/s12249-014-0214-8.

Planinšek, O., Kovačič, B., Vrečer, F., 2011. Carvedilol dissolution improvement by preparation of solid dispersions with porous silica. Int. J. Pharm. 406, 41–48. http://dx.doi.org/10.1016/j.ijpharm.2010.12.035.

Pouton, C.W., Porter, C.J.H., 2008. Formulation of lipid-based delivery systems for oral administration: Materials, methods and strategies. Adv. Drug Deliv. Rev. 60, 625–637. http://dx.doi.org/10.1016/j.addr.2007.10.010.

Renterghem, J., Vervaet, C., De Beer, T., 2017. Rheological characterization of molten polymer-drug dispersions as a predictive tool for pharmaceutical hot-melt extrusion processability. Pharm. Res. 34, 2312–2321. http://dx.doi.org/10.1007/s11095-017-2239-7.

Seo, A., Holm, P., Kristensen, H.G., Schæfer, T., 2003. The preparation of agglomerates containing solid dispersions of diazepam by melt agglomeration in a high shear mixer. Int. J. Pharm. 259, 161–171. http://dx.doi.org/10.1016/S0378-5173(03)00228-X.

Shah, M.K., Madan, P., Lin, S., 2014. Preparation, in vitro evaluation and statistical optimization of carvedilol-loaded solid lipid nanoparticles for lymphatic absorption via oral administration. Pharm. Dev. Technol. 19, 475–485. http://dx.doi.org/10.3109/10837450.2013.795169.

Shamma, R.N., Basha, M., 2013. Soluplus®: a novel polymeric solubilizer for optimization of carvedilol solid dispersions: formulation design and effect of method of preparation. Powder Technol. 237, 406–414. http://dx.doi.org/10.1016/j.powtec.2012.12.038.

Shete, H., Patravale, V., 2013. Long chain lipid based tamoxifen NLC. Part I: preformulation studies, formulation development and physicochemical characterization. Int. J. Pharm. 454, 573–583. http://dx.doi.org/10.1016/j.ijpharm.2013.03.034.

Silva, L.A.D., Cintra, E.R., Alonso, E.C.P., Alves, G.L., Lima, E.M., Taveira, S.F., Cunha-Filho, M.S.S., Marreto, R.N., 2017. Selection of excipients for the development of carvedilol loaded lipid-based drug delivery systems. J. Therm. Anal. Calorim. 130, 1593–1604. http://dx.doi.org/10.1007/s10973-017-6380-7.

Silva, L.A.D., Teixeira, F.V., Serpa, R.C., Esteves, N.L., Santos, R.R., Lima, E.M., Cunha-Filho, M.S.S., Araújo, A.A.S., Taveira, S.F., Marreto, R.N., 2016. Evaluation of carvedilol compatibility with lipid excipients for the development of lipid-based drug delivery systems. J. Therm. Anal. Calorim. 123, 2337–2344. http://dx.doi.org/10.1007/s10973-015-5022-1.

Singh, B., Bandopadhyay, S., Kapil, R., Singh, R., Katare, O.P., 2009. Self-Emulsifying drug delivery systems (SEDDS): formulation development, characterization, and applications. Crit. Rev. Ther. Drug Carrier Syst. 26, 427–521. http://dx.doi.org/10.1615/CritRevTherDrugCarrierSyst.v26.i5.10.

Singh, B., Singh, R., Bandyopadhyay, S., Kapil, R., Garg, B., 2013. Optimized nanoemulsifying systems with enhanced bioavailability of carvedilol. Colloid Surface B 101, 465–474. http://dx.doi.org/10.1016/j.colsurfb.2012.07.017.

Singh, B., Beg, S., Khurana, R.K., Sandhu, P.S., Kaur, R., Katare, O.P., 2014. Recent advances in self-emulsifying drug delivery systems (SEEDS). Crit. Rev. Ther. Drug

Carrier Syst. 31, 121–185. http://dx.doi.org/10.1615/CritRevTherDrugCarrierSyst.2014008502.

Stanković, M., Frijlink, H.W., Hinrichs, W.L.J., 2015. Polymeric formulations for drug release prepared by hot melt extrusion: application and characterization. Drug Discov. Today 20, 812–823. http://dx.doi.org/10.1016/j.drudis.2015.01.012.

Tan, A., Rao, S., Prestidge, C.A., 2013. Transforming lipid-based oral drug delivery systems into solid dosage forms: an overview of solid carriers, physicochemical properties, and biopharmaceutical performance. Pharm. Res. 30, 2993–3017. http://dx.doi.org/10.1007/s11095-013-1107-3.

Tang, B., Cheng, G., Gu, J.-C., Xu, C.-H., 2008. Development of solid self-emulsifying drug delivery systems: preparation techniques and dosage forms. Drug Discov. Today 13, 606–612. http://dx.doi.org/10.1016/j.drudis.2008.04.006.

Thiry, J., Krier, F., Evrard, B., 2015. A review of pharmaceutical extrusion: Critical process parameters and scaling-up. Int. J. Pharm. 479, 227–240. http://dx.doi.org/10.1016/j.ijpharm.2014.12.036.

Venishetty, V.K., Chede, R., Komuravelli, R., Adepu, L., Sistla, R., Diwan, P.V., 2012. Design and evaluation of polymer coated carvedilol loaded solid lipid nanoparticles to improve the oral bioavailability: a novel strategy to avoid intraduodenal administration. Colloid Surf. B 95, 1–9. http://dx.doi.org/10.1016/j.colsurfb.2012.01.001.

Wang, Z., Sun, J., Wang, Y., Liu, X., Liu, Y., Fu, Q., Meng, P., He, Z., 2010. Solid self-emulsifying nitrendipine pellets: preparation and *in vitro/in vivo* evaluation. Int. J. Pharm. 383, 1–6. http://dx.doi.org/10.1016/j.ijpharm.2009.08.014.

Wei, L., Sun, P., Nie, S., Pan, W., 2005. Preparation and evaluation of SEDDS and SMEDDS containing carvedilol. Drug Dev. Ind. Pharm. 31, 785–794. http://dx.doi.org/10.1080/03639040500216428.

Wessler, J.D., Grip, L.T., Mendell, J., Giugliano, R.P., 2013. The P-glycoprotein transport system and cardiovascular drugs. J. Am. Coll. Cardiol. 61, 2495–2502. http://dx.doi.org/10.1016/j.jacc.2013.02.058.

Yi, T., Wan, J., Xu, H., Yang, X., 2008. A new solid self-microemulsifying formulation prepared by spray-drying to improve the oral bioavailability of poorly water soluble drugs. Eur. J. Pharm. Biopharm. 70, 439–444. http://dx.doi.org/10.1016/j.ejpb.2008.05.001.

Zecevic, D.E., Meier, R., Daniels, R., Wagner, K.-G., 2014. Site specific solubility improvement using solid dispersions of HPMC-AS/HPC SSL – mixtures. Eur. J. Pharm. Biopharm. 87, 264–270. http://dx.doi.org/10.1016/j.ejpb.2014.03.018.